THE JOURNAL OF BIOLOGICAL CHEMISTRY VOL. 290, NO. 13, pp. 8154–8165, March 27, 2015

The Intracellular Domain of Teneurin-1 Induces the Activity of Microphthalmia-associated Transcription Factor (MITF) by Binding to Transcriptional Repressor HINT1

Received for publication, October 1, 2014, and in revised form, February 2, 2015 Published, JBC Papers in Press, February 3, 2015, DOI 10.1074/jbc.M114.615922

Jonas Schöler[‡§], **Jacqueline Ferralli**[‡], **Stéphane Thiry**[‡], **and Ruth Chiquet-Ehrismann**[‡§1]

From the [‡]*Friedrich Miescher Institute for Biomedical Research, Maulbeerstrasse 66, 4058 Basel, Switzerland and the* [§]*Faculty of Science, University of Basel, Klingelbergstrasse 50, 4056 Basel, Switzerland*

Background: The intracellular domain of teneurins translocates to the nucleus and is thought to influence transcription.
Results: The teneurin-1 intracellular domain binds the transcriptional repressor HINT1 and induces MITF target genes.
Conclusion: The teneurin-1 intracellular domain prevents HINT1 from repressing MITF at its target gene promoters.
Significance: This is a novel mechanism for a teneurin-mediated transcriptional control.

Teneurins are large type II transmembrane proteins that are necessary for the normal development of the CNS. Although many studies highlight the significance of teneurins, especially during development, there is only limited information known about the molecular mechanisms of function. Previous studies have shown that the N-terminal intracellular domain (ICD) of teneurins can be cleaved at the membrane and subsequently translocates to the nucleus, where it can influence gene transcription. Because teneurin ICDs do not contain any intrinsic DNA binding sequences, interaction partners are required to affect transcription. Here, we identified histidine triad nucleotide binding protein 1 (HINT1) as a human teneurin-1 ICD interaction partner in a yeast two-hybrid screen. This interaction was confirmed in human cells, where HINT1 is known to inhibit the transcription of target genes by directly binding to transcription factors at the promoter. In a whole transcriptome analysis of BS149 glioblastoma cells overexpressing the teneurin-1 ICD, several microphthalmia-associated transcription factor (MITF) target genes were found to be up-regulated. Directly comparing the transcriptomes of MITF *versus* TEN1-ICD-overexpressing BS149 cells revealed 42 co-regulated genes, including glycoprotein non-metastatic b (*GPNMB*). Using real-time quantitative PCR to detect endogenous *GPNMB* expression upon overexpression of MITF and HINT1 as well as promoter reporter assays using *GPNMB* promoter constructs, we could demonstrate that the teneurin-1 ICD binds HINT1, thus switching on MITF-dependent transcription of *GPNMB*.

Teneurins are a well conserved protein family that were originally identified in *Drosophila* (1–3). Whereas two paralogs have been described in the fruit fly and one in *Caenorhabditis elegans*, four members, namely teneurins 1–4, have been identified in vertebrates (4, 5). Expression patterns during development taken together with functional studies strongly suggest a role for teneurins during development of the CNS in *Drosophila* (6–8), *C. elegans* (9, 10), chicken (6, 11–15), and mouse (5, 16–19), although teneurins are likely to play roles in other regions, like the developing limbs, as well (12, 13).

Members of this protein family are type II transmembrane proteins containing a single-spanning transmembrane domain. Teneurins are about 300 kDa in size, the largest part being the C-terminal extracellular domain (ECD),[2] which contains several conserved domains (11). Following the transmembrane domain, many teneurins have furin cleavage sites (20) preceding eight EGF repeats, through which teneurins can dimerize due to free cysteines in repeats 2 and 5 forming interchain disulfide bonds (5, 21). The following NHL repeat domain is a predicted β-propeller and is responsible for homophilic rather than heterophilic interactions in some teneurins (5, 22), although heterophilic interactions have also been observed (23). Interestingly, these interactions can lead to the release of the ECD (11, 24). Further, there are 26 YD repeats, which are unique for a eukaryotic protein because they are generally found in bacterial cell wall proteins (4). Finally, the most C-terminal domain or teneurin C-terminal associated peptide has been described as having sequence similarity to corticotropin-releasing factor (25) and has neuromodulatory activity (26). More recently striking homology of the C-terminal half of the teneurin ECDs, including the NHL, YD, and teneurin C-terminal associated peptide regions, was discovered with bacterial ABC toxins (27, 28).

The N-terminal intracellular domain is about 45 kDa in size and is not as conserved across all phyla as the ECD (6, 29). Nevertheless, vertebrate ICDs share a sequence similarity of up to 70% between orthologs and 50–60% between paralogs, and the ICDs contain several common features and domains. There is an EF-hand-like Ca^{2+} binding site, predicted phosphoryla-

The data reported in this paper have been deposited in the Gene Expression Omnibus (GEO) database, www.ncbi.nlm.nih.gov/geo (accession nos. 61704 and 61705).

[1] To whom correspondence should be addressed: Novartis Research Foundation, Friedrich Miescher Institute for Biomedical Research, Maulbeerstrasse 66, 4058 Basel, Switzerland. E-mail: ruth.chiquet@fmi.ch.

[2] The abbreviations used are: ECD, extracellular domain; ICD, intracellular domain; qPCR, quantitative PCR; IPA, ingenuity pathway analysis; GBD, glucocorticoid binding domain; Dox, doxycycline; Dex, dexamethasone; SEAP, secreted embryonic alkaline phosphatase; tet, tetracycline; MITF, microphthalmia-associated transcription factor.

tion sites, and polyproline-rich regions shown to bind SH3 domain-containing proteins like CAP/Ponsin (29, 30).

Teneurins were first identified as pair-rule genes (2, 3), which was curious because pair-rule genes were known to be transcription factors rather than transmembrane proteins (5). Although this evidence was recently refuted (31), it still paved the way to implicate the teneurin ICDs in transcriptional regulation. Regulated intramembrane proteolysis by either site-2 protease, signal peptide peptidase, or signal peptide peptidase-like proteases is predicted to release the ICD (24) before it translocates to the nucleus, as shown by several *in vitro* and *in vivo* studies (14, 29, 32). In the nucleus, the teneurin-2 ICD affects zic-mediated transcription and is localized to PML bodies, which are so-called transcriptional hotspots (32). The teneurin-1 ICD can bind to MBD1, a transcriptional repressor (29). Interaction partners are crucial for the ICDs to influence transcriptional regulation because they do not contain any intrinsic DNA binding sequences.

Although the teneurin ICDs are strongly implicated in transcriptional regulation, target genes as well as mechanisms have yet to be elucidated. In this study, we are investigating the transcriptional activity of the human teneurin-1 ICD, which will be referred to as simply TEN1-ICD hereafter. We performed two unbiased screens to identify 1) interacting proteins and 2) target genes involved in the transcriptional control of these target genes. We will show how the ICD can influence transcription via HINT1, a transcriptional repressor that directly binds to transcription factors at the promoters of their target genes (33, 34).

EXPERIMENTAL PROCEDURES

Cloning—All constructs were prepared by classical cloning procedures and verified by sequencing. TEN1-ICD was cloned from human adult brain cDNA (20), HINT1 from pPR3-N-HINT1 (Dualsystems), eGFP-His from pcDNA3-EGFP (Addgene), RFP-HA from pQCXIX-RFP (Clontech), CFP-MYC from pECFP1-C1 (Addgene), and MITF from pCMV6-MITF variant 4 (Origene). The following constructs were prepared in pcDNA3 (Invitrogen): HINT1-MYC, TEN1-ICD-HA, HINT1-CFP-MYC, RFP-HA, and MITF-RFP-HA (note that all tags are C-terminal). For inducible overexpression studies with the TEN1-ICD, we used the highly predictable and tightly regulated gene expression system described by Anastassiadis *et al.* (35) using the following plasmids: pirtetR-GBD as tetracycline (tet) activator plasmid and eGFP-His and TEN1-ICD-eGFP-His in the tet promoter plasmid ptetO as described previously (35). For the yeast two-hybrid screen, TEN1-ICD was cloned into pDHB1 (Dualsystems). For promoter reporter studies, the *GPNMB* and *GPNMB* ΔM-box promoters were cloned into pSEAP2basic (Clontech). Promoter sequences *GPNMB* (1096 bp) and *GPNMB* ΔM-box (144 bp) as described (36) were cloned from HT1080 cell whole genomic DNA and extracted with the DNeasy tissue kit (Qiagen) using the following primers: ACTAGCTAGCGCCACATTTTCTGCATACTCTG (forward) and ACTACTCGAGCATCTGTGGTGCCTCCCTCT (reverse) and ATGCTAGCGAACTTGAGAGACCAGATCAGGC (forward) and ATCTCGAGCAGTGTTCTTCTGGCATCTGTGGTGCCTCCCTCTC (reverse), respectively.

Cell Culture—BS149, SH-SY5Y, U373, LN229, MO95S, U343MG, and T98G cells (kind gift of the Hemmings laboratory at the Friedrich Miescher Institute for Biomedical Research) and COS-7 (ATCC) cells were cultured in DMEM containing 10% fetal bovine serum (FBS), 100 mg/liter penicillin, and 100 mg/liter streptomycin. Genes were either overexpressed by transient transfection or by a modified tet system kindly provided by Gerrit Fischedick of the Schöler laboratory at the Max Planck Institute for Molecular Biomedicine (35). Cells were transfected with jetPEI (Polyplus). BS149 cells were first transfected with pirtetR-GBD and made stable by 0.5 μg/μl puromycin selection and then, after further transfection with either ptetO-eGFP-His or ptetO-TEN1-ICD-eGFP-His, by 150 μg/μl hygromycin selection. The tet system was induced by adding 10^{-7} M dexamethasone (Dex) 100% ethanol and 1 μg/ml doxycycline (Dox) in Milli-Q water to the medium.

Yeast Two-hybrid Screen—The yeast two-hybrid screen was performed using the DUALhunter starter kit (Dualsystems) and following its manual. Prey proteins were fished with the bait protein TEN1-ICD, out of the normalized human fetal brain cDNA (NubG-X) library (Dualsystems).

Proximity Ligation Assay and Immunocytochemistry—The proximity ligation assay was performed using the DUOlink system (Sigma-Aldrich) and following the appropriate protocol provided by the manufacturer. COS-7 cells were transfected with either HINT1-MYC as negative control or both HINT1-MYC and TEN1-ICD-HA to identify an interaction. For detection, mouse monoclonal α-HA (42F13, used as hybridoma supernatant) and rabbit polyclonal α-MYC (Abcam) antibodies were used. For immunocytochemistry, parallel cultures were stained with the same primary antibodies and Alexa Fluor 488 goat anti-rabbit and Alexa Fluor 568 goat anti-mouse (both from Life Technologies) as secondary antibodies. Cells were viewed with an Axioskop 50 microscope (Zeiss), and pictures were taken with an ORCA-ER digital camera (Hamamatsu).

Real-time qPCR—To determine endogenous transcript levels of teneurin-1 in normal tissues, brain total RNA, fetal brain RNA, and cerebellum RNA were acquired (Clontech). For the glioblastoma cell line screen of endogenous teneurin-1 expression, 1×10^6 cells were used for RNA extraction. Experiments were performed in biological triplicates, where for each cell line RNAs were extracted from independent cultures on three consecutive days. All overexpressing cells were FACS-sorted directly into RLT lysis buffer (Qiagen) at a 3:1 volume ratio of lysis buffer to cells in PBS, 24 h after induction or transfection. Total RNA was extracted with an RNeasy Mini kit and QIAshredder columns (both from Qiagen) and reverse-transcribed into cDNA, using random hexamer primers with the high capacity cDNA reverse transcription kit (Applied Biosystems).

For real-time qPCR, gene-specific primers (Table 1) were designed, and all data were normalized to TBP, using Platinum SYBR Green qPCR SuperMix-UDG with ROX (Invitrogen) on a StepOnePlus real-time PCR system (Applied Biosystems). Endogenous levels were calculated by using the comparative C_T method (37).

Western Blot—BS149 cells were induced or kept uninduced as a negative control at 70% confluence on a 3.5-cm plate and

TABLE 1
Real-time qPCR primers
Shown are human primers for all real-time qPCR experiments, using Platinum SYBR Green qPCR SuperMix-UDG with ROX.

Target	Forward primer	Reverse primer
Teneurin-1 ICD	CTACCTGGATTTCCCAAACC	CCAGGATAGTCTTTCCAGGA
Teneurin-1 ECD	GCATAGTTCCTGTTTGTCCA	TCTGCACATCTTGAGTAGAC
Teneurin-1 ICD-GFP	GAAGCACCTTTTCCCGACCT	CGGACACGCTGAACTTGTG
GPNMB	AAGTGAAAGATGTGTACGTGGTAACAG	TCGGATGAATTTCGATCGTTCT
SCARB1	AATAAGCCCATGACCCTGAAGC	GCCCCACATGATCTCACCC
EDNRB	CTGCTGCACATCGTCATTGAC	GCTCCAAATGGCCAGTCCT
SLC1A4	CAGCGACCCTTCCCTCTATGA	GCCCCGATGGGGAGAATAAAC
SEMA6A	ACATTGCTGCTAGGGACCATA	TCTGCATGTGTCTACATCGGC
ERBB3	GTCTGTGTGACCCACTGCAACT	GGGTGGCAGGAGAAGCATT
CHL1	ACCAACATTTTCGTGGACTAAGG	TCGATGGAATTATCCGATGGTCA
TBP	TGCACAGGAGCCAAGAGTGAA	CACATCACAGCTCCCCACCA

harvested after 24 h directly in sample buffer, containing β-mercaptoethanol. Samples were run on a 10% polyacrylamide gel and blotted on a PVDF membrane. Protein bands were detected by a mouse monoclonal α-GFP antibody (Roche Applied Science) in 5% skim milk in 1× TBS-Tween 20 (0.05%), a mouse monoclonal α-vinculin antibody (Sigma-Aldrich) as a loading control, and a goat α-mouse secondary horseradish peroxidase-conjugated antibody (Invitrogen) with SuperSignal West Dura Chemiluminescent Substrate (Thermo Scientific).

Microarray—For the whole transcriptome analysis of TEN1-ICD overexpression, the stable BS149 cell lines with pirtetR-GBD/ptetO-eGFP-His or pirtetR-GBD/ptetO-TEN1-ICD-eGFP-His were split into three 10-cm Petri dishes each. The triplicate cell lines were cultured once before induction with Dex and Dox. For the whole transcriptome analysis of MITF, cells were transiently transfected in triplicates with either pcDNA3-RFP-HA or pcDNA3-MITF-RFP-HA. The overexpressing cells were then FACS-sorted directly into RLT lysis buffer (Qiagen) at a 3:1 volume ratio of lysis buffer to cells in PBS, 24 h after induction or transfection. Total RNA was extracted with an RNeasy Mini kit and QIAshredder columns (both from Qiagen) and reverse-transcribed into cDNA, using random hexamer primers with the high capacity cDNA reverse transcription kit (Applied Biosystems). 100 ng of extracted total RNA was amplified using the Ambion WT expression kit (Ambion), and the resulting sense strand cDNA was fragmented and labeled using the Affymetrix GeneChip WT terminal labeling kit (Affymetrix). Affymetrix gene chip arrays were hybridized following the "GeneChip Whole Transcript (WT) Sense Target Labeling Assay Manual" (Affymetrix) with a hybridization time of 16 h. The Affymetrix Fluidiscs protocol FS450_0007 was used for washing. Scanning was performed with Affymetrix GCC Scan Control version 3.0.0.1214 on a GeneChip Scanner 3000 with autoloader. Arrays were normalized, and probe set level expression values were calculated with the R/Bioconductor (version 2.14) "affy" package using the rma() function. Differential gene expression was calculated with the Bioconductor package limma using a linear -fold change cut-off = 1.5 and a Benjamini-Hochberg corrected p value = 0.05. For volcano plots, log2 -fold changes were plotted against the log10 (adjusted p value) in R (version 3.1.1). Significantly differentially expressed genes are marked in *blue*, and genes of interest are labeled in *red*. Normalized unscaled expression values for the genes passing these filters were plotted using the heatmap.2() function of the gplots package.

Ingenuity Pathway Analysis (IPA)—Normalized unscaled expression values for the genes passing -fold change cut-off = 1.5 and a Benjamini-Hochberg corrected p value = 0.05 filter were up-loaded into IPA (Qiagen) and run through the pathway analysis. The upstream analysis was filtered for transcriptional regulators and sorted by activation z-score. The MITF network was created via the My Pathways option, only allowing direct connections related to transcriptional regulation.

SEAP Reporter Assays—Promoter reporter assays were performed by cotransfecting BS149 cells with 1 μg of pSEAP2basic-promoter constructs and either 0.5 μg of empty pcDNA3 vector, 0.5 μg of MITF, 0.05 μg of MITF plus 0.45 μg of empty pcDNA3 vector, or 0.05 μg MITF plus 0.45 μg of TEN1-ICD and 150 ng of the *Metridia* luciferase pMetLuc reporter vector (Clontech) for the normalization of the transfection efficiency. SEAP activity measurements were taken 24 h post-transfection by using the chemiluminescent SEAP reporter gene assay (Roche Applied Science). The *Metridia* luciferase assay for normalization was performed with the Ready-to-Glow secreted luciferase reporter assay (Clontech). All values were measured by the Mithras LB940 Luminometer (Berthold Technologies).

Statistical Analysis—All grouped data are means ± S.D. Statistical analysis was completed using GraphPad InStat version 3.05. Differences between two groups were evaluated using a two-tailed Student's t test for parametric data or a Mann-Whitney U test for nonparametric data. Multiple comparisons were performed using one-way analysis of variance. Values of $p < 0.05$ were considered statistically significant.

RESULTS

Identification of TEN1-ICD Interaction Partners—To identify new interaction partners, we performed a yeast two-hybrid screen using the TEN1-ICD as a membrane-anchored bait protein fishing for prey encoded by a human fetal brain cDNA library. The benefit of this method is that baits that might activate transcription independently of a prey are prevented from entering the nucleus, making them nevertheless usable for a screen. Furthermore, the readout is based on the split ubiquitin method, in which an interaction of the bait and prey proteins also joins the N- and C-terminal parts of split ubiquitin. A ubiquitin-specific protease then releases the artificial transcription factor LexA-VP16 to switch on the two reporters HIS3 and LacZ (Fig. 1*A*). The yeast strain NMY51 can thus grow on a defined minimal medium lacking histidine only when an inter-

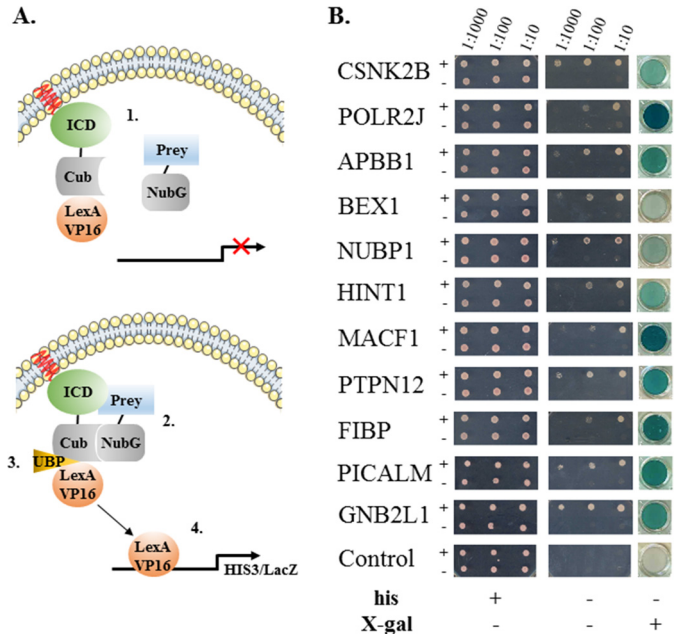

FIGURE 1. **Novel interaction partners of teneurin-1 ICD identified by yeast two-hybrid screen.** *A*, DUALhunter yeast two-hybrid screen. *1*, when the teneurin-1 ICD (bait protein) and the prey protein do not interact, the reporter genes are not expressed. *2*, once an interaction takes place, the C- and N-terminal parts of split ubiquitin are united. *3*, a ubiquitin-specific protease releases the attached transcription factor. *4*, the transcription factor switches on expression of the HIS3/LacZ reporters. *B*, interaction partners identified by the screen. *Left*, serial dilutions of yeast strain NMY51 transformed with the prey-NubG plasmid or an empty prey-NubG plasmid (*Control*), together with either the membrane-anchored bait plasmid TEN1-ICD-Cub-LexA-VP16 (+) or the membrane-bound empty bait plasmid Cub-LexA-VP16 (−) grown on −Trp/−Leu medium containing histidine. *Center*, the same dilutions of the transformed NMY51 yeast as shown on the *left*, grown on medium lacking histidine, thus showing growth only if an interaction between bait and prey proteins took place. *Right*, β-galactosidase assay of yeast transformed with the bait TEN1-ICD-Cub-LexA-VP16 together with the prey plasmids indicated or with an empty prey plasmid (*Control*).

action occurs and turns the medium blue due to β-galactosidase cleaving added X-Gal. Our screen resulted in the isolation of more than 100 positive colonies, and their bait plasmids were isolated and sequenced. The isolated plasmids were retransformed into NMY51 together with the TEN1-ICD or the empty prey plasmid and tested at different dilutions for growth on medium lacking histidine (Fig. 1*B*). The positive controls show that the yeast do contain all plasmids and grow when the defined minimal medium contains histidine, and no interaction is required between bait and prey proteins for their growth (Fig. 1*B*, *left*). When the medium lacks histidine, there is a robust growth of the NYM51 colonies only when the bait and prey proteins interact (Fig. 1*B*, *right*). There is also a *blue coloration* for all candidates in the β-galactosidase assay (Fig. 1*B*). We thus identified a total of 11 interaction partners, each being potentially interesting in the context of teneurin function. The main features of each interacting protein are summarized in Table 2.

Several MITF Target Genes Are Up-regulated in TEN1-ICD-overexpressing Cells—In parallel, we wanted to identify a system to study how the overexpression of the TEN1-ICD influences transcription, assuming that cells with endogenous teneurin-1 expression also have the machinery to respond to teneurin-1 signaling. To get started, we performed a qPCR screen identifying glioblastoma cell lines that express endogenous teneurin-1 (Fig. 2*A*, *left*). We chose the BS149 cell line for our further studies because it has an endogenous expression of teneurin-1 and excellent transfection efficiency. We also compared the levels of TEN-1 transcripts in BS149 cells to tissues known to express teneurins, such as the brain. Whereas total adult brain RNA contained about 18.3-fold more teneurin-1 transcripts, the levels in fetal brain and adult cerebellum were 50.5- and 181.7-fold higher, respectively, than in BS149 cells (Fig. 2*A*, *right*).

To study the influence of teneurin-1 on transcriptional regulation in BS149 cells, we needed an inducible method to overexpress the TEN1-ICD transiently. Thus, we used a modified and improved tet system, which eliminates the leakiness of the promoter (35). Two separate vectors are required to make the cell line stable (Fig. 2*B*). One contains the tet-activating domain fused to a glucocorticoid binding domain (GBD). The other contains the tetO operator sequences directly upstream of a CMV promoter and the gene to be overexpressed. The tet-activating domain is continuously expressed and bound to HSP90 in the cytosol via the GBD. Adding Dex releases the fusion protein from HSP90 and subsequently binds the tetO-CMV promoter, switching on gene expression due to the addition of Dox. This system allows for well controlled induction of transcripts in a physiological range. First, we were able to show the functionality of the system by Western blot of cell extracts of the stable BS149 cells induced by Dex/Dox addition. TEN1-ICD-eGFP-His and eGFP-His fusion proteins were detected only when the modified tet system was induced (Fig. 2*C*). qPCR confirmed the specific overexpression of the TEN1-ICD-eGFP-His fusion construct, resulting in a 214.9-fold increase, compared with endogenous teneurin-1 expression, on a transcript level (Fig. 2*D*). Although this might appear as very strong overexpression, this is not more than is observed in total RNA of adult cerebellum. Thus, at least on a transcript level, the overexpressed TEN1-ICD is in a physiological range.

To show the effects on transcriptional regulation in BS149 cells, we overexpressed the TEN1-ICD-eGFP-His construct by induction of the tet system and compared it with the overexpression of the eGFP-His construct in a whole transcriptome microarray analysis. For more rigorous results, we compared biological triplicates and separately induced and FACS-sorted the cells for GFP expression before extraction of their total RNA. With a -fold change cut-off excluding values below 1.5 and an adjusted *p* value cut-off excluding values above 0.05, we obtained a list of 430 differentially regulated genes. An upstream pathway analysis by IPA was used to identify the top 20 transcriptional regulators with a significant number of downstream targets in the data set (Table 3). The list was sorted based on positive activation *z*-scores (*i.e.* these transcriptional regulators are all activated). One of the transcriptional regulators in the list, MITF, is a well described basic helix-loop-helix leucine zipper transcription factor that has previously been shown to be directly inhibited by the histidine triad nucleotide-binding protein HINT1 (33, 34). Interestingly, HINT1 was one of the interaction partners found in the yeast two-hybrid screen described above, and we considered that this interaction may be involved in the induction of MITF target genes by the TEN1-ICD.

TABLE 2

Teneurin-1 ICD interaction partners

Information about all interaction partners of the TEN1-ICD, as identified in the yeast two-hybrid screen.

Gene	Protein name	Information
CSNK2B	Casein kinase II subunit β	Regulatory subunit of casein kinase II (CK2); not required for catalytic activity; recruits substrates/ regulators; CK2 is a pleiotropic kinase involved in *e.g.* cell proliferation, transcription, etc. (59)
POLR2J	DNA-directed RNA polymerase II subunit RPB11-a	Subunit of the RNA polymerase II complex; forms heterodimer with POLR2C, which is part of the core enzyme; involved in the termination of transcription; binds to SATB1 and Che-1 (60–62)
APBB1	Amyloid β A4 precursor protein-binding family B member 1	Adapter protein; aids in processing of amyloid precursor protein (APP) by binding to it; this interaction also influences production of amyloid-β peptides that are found in Alzheimer patients; promotes neurite outgrowth (63)
BEX1	Brain-expressed X-linked protein 1	Small adapter protein; involved in NGFR signaling and transcriptional regulation of cell cycle arrest genes; implicated in promoting survival of neurons and neurite outgrowth (51, 52)
NUBP1	Nucleotide binding protein 1	MRP/MinD-type P-loop NTPase; interacts with motor protein KIFC5A; involved in regulation of centriole duplication; implicated in assembly of cytosolic iron-sulfur proteins (64)
HINT1	Histidine triad nucleotide-binding protein 1	Member of the evolutionarily conserved HIT superfamily; tumor suppressor gene; inhibits transcription factors like MITF and β-catenin by directly binding them at the promoters of their target genes (34)
MACF1	Microtubule-actin cross-linking factor 1	Spectraplakin and + TIP protein; conserved SH3 domain; role in cross-linking microtubules to actin cytoskeleton; regulates growth of neuronal microtubules, and subsequently filopodia formation and axon extension (53, 54)
PTPN12	Tyrosine-protein phosphatase non-receptor type 12	Part of non-receptor PTP subfamily; ubiquitously expressed phosphatase; important functions in early embryogenesis, like development of mesenchyme; involved in cell spreading and migration (65)
FIBP	Acidic fibroblast growth factor intracellular binding protein	Selectively binds aFGF; implicated in mitogenic action of aFGF; up-regulated in some cancers; involved in angiogenesis of tumors (66, 67)
PICALM	Phosphatidylinositol-binding clathrin assembly protein	Ubiquitously expressed adapter protein; strongest expression in neurons, especially in pre- and postsynaptic structures; risk factor for Alzheimer disease; plays a role in clathrin-mediated endocytosis (68, 69)
GNB2L1	Guanine nucleotide-binding protein	Scaffold protein; originally identified as anchoring protein for protein kinase C; also recruits and binds other proteins like integrins; altered expression levels in many cancers (70)

The relationships of MITF to its downstream targets are shown in an IPA My Pathways network. Seven of the eight target genes present in this database are consistently up- or down-regulated in our microarray experiment, with only the exception of *NGFR* (Fig. 3). A literature search revealed three further positively regulated MITF target genes in our microarray data, *ERBB3*, *SLC1A4*, and *CHL1* (38). All target genes are marked in a *volcano plot* (Fig. 4*A*), summarizing the microarray data. Consistent up- or down-regulation of the MITF target genes in the triplicates of the microarray is shown in Fig. 4*B* and was confirmed for some of the target genes by qPCR (Fig. 4*C*). To exclude the possibility that these target genes are a result of the particular stable cell line used for the transcript profiling, we created a second set of stable BS149 cell lines using the same vectors of the modified tet system. Again, we confirmed all target genes by qPCR (data not shown).

Proximity Ligation Assay Confirms Interaction of TEN1-ICD and HINT1—To confirm the interaction between HINT1 and TEN1-ICD not only in yeast but also in human cells, we recloned *HINT1* with a MYC tag into a mammalian expression vector. We used the proximity ligation assay to test whether the proteins interact when expressed in COS-7 cells. We co-transfected vectors encoding HINT1-MYC and TEN1-ICD-HA; if the two proteins are located in close proximity to each other, the oligonucleotides present on the secondary antibodies used to detect the two proteins can hybridize and be ligated and amplified using fluorescence-labeled nucleotides. Immunocytochemistry images of co-transfected cells show that many COS-7 cells overexpress both proteins in the cytoplasm as well as in the nucleus (Fig. 5*A*). Using a proximity ligation assay, the HINT1-MYC and TEN1-ICD-HA co-transfection confirms an interaction, as seen by the fluorescent red dots in the cells that are overexpressing both proteins (Fig. 5*B*, *left* and *center image*). As a negative control, the same primary and secondary antibodies were used, but only HINT1-MYC was overexpressed in COS-7 cells (Fig. 5*B*, *right image*). Therefore, we concluded that the TEN1-ICD indeed binds to HINT1, and we hypothesized that the TEN-1 ICD might act by sequestering HINT1, thereby compromising its repression of MITF-mediated transcription.

GPNMB Is Co-regulated by the TEN1-ICD, MITF, and HINT1—If our hypothesis is correct and there is a connection between the TEN1-ICD and MITF in regulating transcription

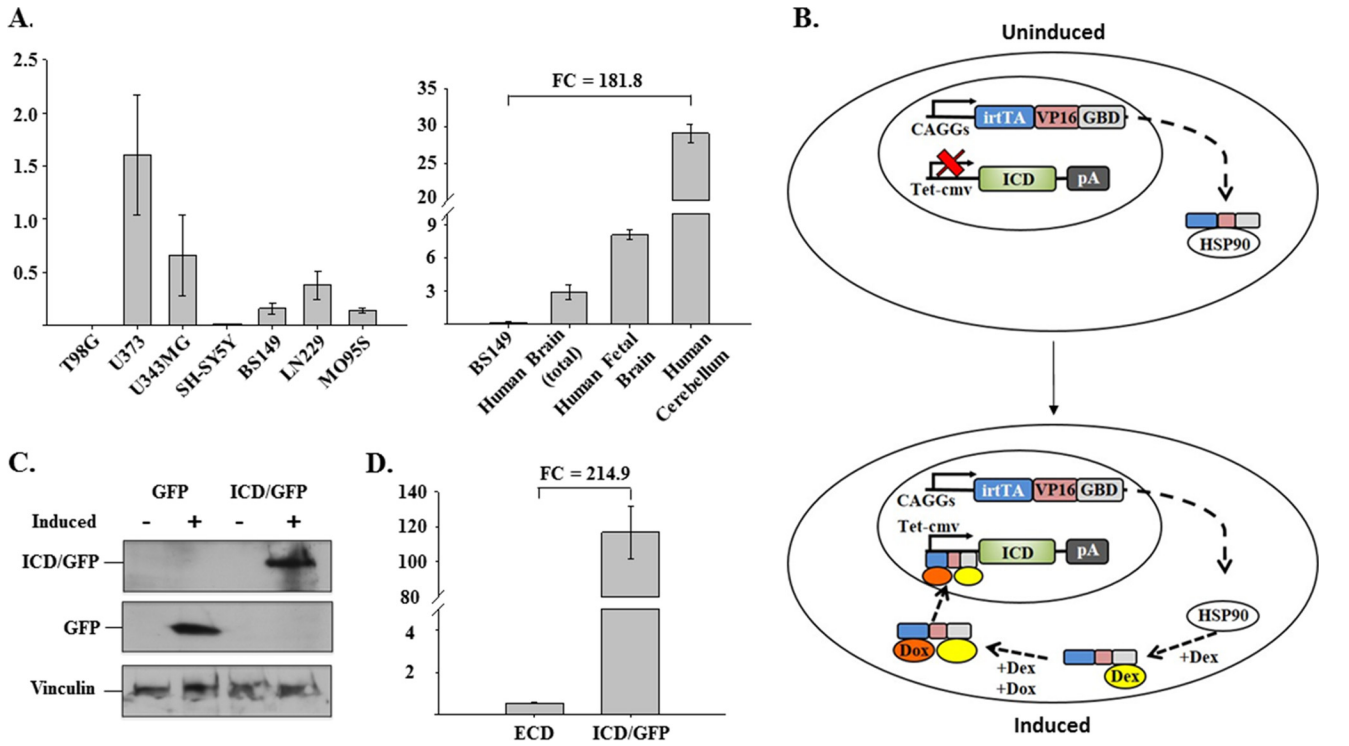

FIGURE 2. **Overexpression of the teneurin-1 ICD through a modified tet system in BS149 cells, a cell line expressing endogenous teneurin-1.** *A*, *left*, quantitative RT-PCR screen of teneurin-1 expression in glioblastoma cell lines. Values are normalized to TBP, using the comparative C_T method. *Right*, quantitative RT-PCR results of teneurin-1 expression comparing the glioblastoma cell line BS149 with different brain tissues. Values are normalized to TBP, using the comparative C_T method. Note that teneurin-1 transcript levels in cerebellum are 181.8-fold higher than in BS149 cells. *B*, scheme of the modified tet system. Through the addition of Dex and Dox, the tet activator construct (irtTA/VP16/GBD) is released from HSP90 in the cytosol and induces expression of the ICD through the tet-CMV promoter. *C*, Western blot with anti-GFP showing the expression of the control construct GFP-His and the teneurin-1 ICD-GFP-His 24 h after the addition of Dex and Dox. Anti-vinculin is the internal control for equal loading. *D*, quantitative RT-PCR results show increased levels of the ICD-GFP fusion construct (using teneurin-1 ICD-GFP primers) compared with endogenous teneurin-1 levels (using teneurin-1 ECD primers) in BS149 cells overexpressing the ICD-GFP construct by a modified tet system, using cDNA prepared from the RNA used in the microarray. Values were normalized to TBP, using the comparative C_T method. Note that teneurin-1 ICD transcript levels are 214.9 times higher than endogenous teneurin-1, which is in the range of the endogenous teneurin-1 present in cerebellum. *Error bars*, S.D.

TABLE 3

Predicted activated transcriptional regulators

IPA upstream pathway analysis list, filtered for transcriptional regulators, sorted by positive activated *z*-score, showing the top 20 results.

Transcriptional regulator	Activation *z*-score	*p* value of overlap	Number of downstream targets in data set
SREBF1	3.872	5.60E − 12	23
SREBF2	3.342	1.85E − 13	17
IRF5	2.415	1.49E − 03	6
STAT2	2.412	1.42E − 04	6
SIRT2	2.236	2.75E − 05	5
NKX2–1	2.224	5.23E − 05	13
PPARGC1B	2.209	4.97E − 06	8
IRF3	2.122	3.51E − 02	7
MYOD1	2.000	3.62E − 02	8
KLF2	1.977	8.46E − 03	8
CEBPD	1.964	5.16E − 04	8
MITF	1.913	1.45E − 02	8
BCL6	1.849	3.44E − 04	10
MYCN	1.830	2.75E − 01	7
IRF1	1.807	6.12E − 05	12
IRF7	1.719	1.40E − 05	13
STAT1	1.677	4.88E − 09	22
BRCA1	1.660	5.48E − 07	15
EGR2	1.633	6.83E − 04	10
NFATC2	1.510	7.29E − 04	10

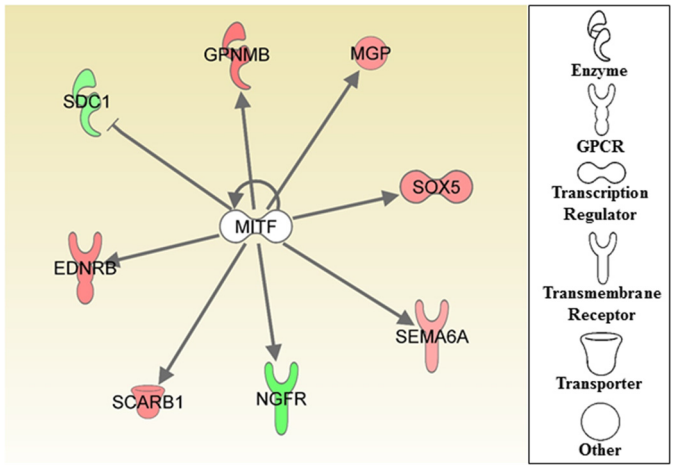

FIGURE 3. **Teneurin-1 ICD overexpression affects MITF target genes.** IPA identified all of its eight MITF target genes in our microarray to be differentially regulated, six up-regulated (*red*) and two down-regulated (*green*). The *arrows* indicate that all genes are directly activated or inhibited by MITF. The regulation of these target genes is consistent with the database for all genes except for *NGFR*, which according to IPA is up-regulated by MITF but is down-regulated in our microarray.

in BS149 cells, MITF overexpression should result in the induction of genes in common with TEN1-ICD induction. To determine the overlap of differentially regulated genes, the MITF-RFP-HA construct was transiently overexpressed in BS149 cells and compared with RFP-HA in a whole transcriptome microarray analysis. Again, we compared biological triplicates by separately transfecting and sorting the cells and extracting their total RNA. With a -fold change cut-off (excluding values below 1.5) and an adjusted *p* value cut-off (excluding values above

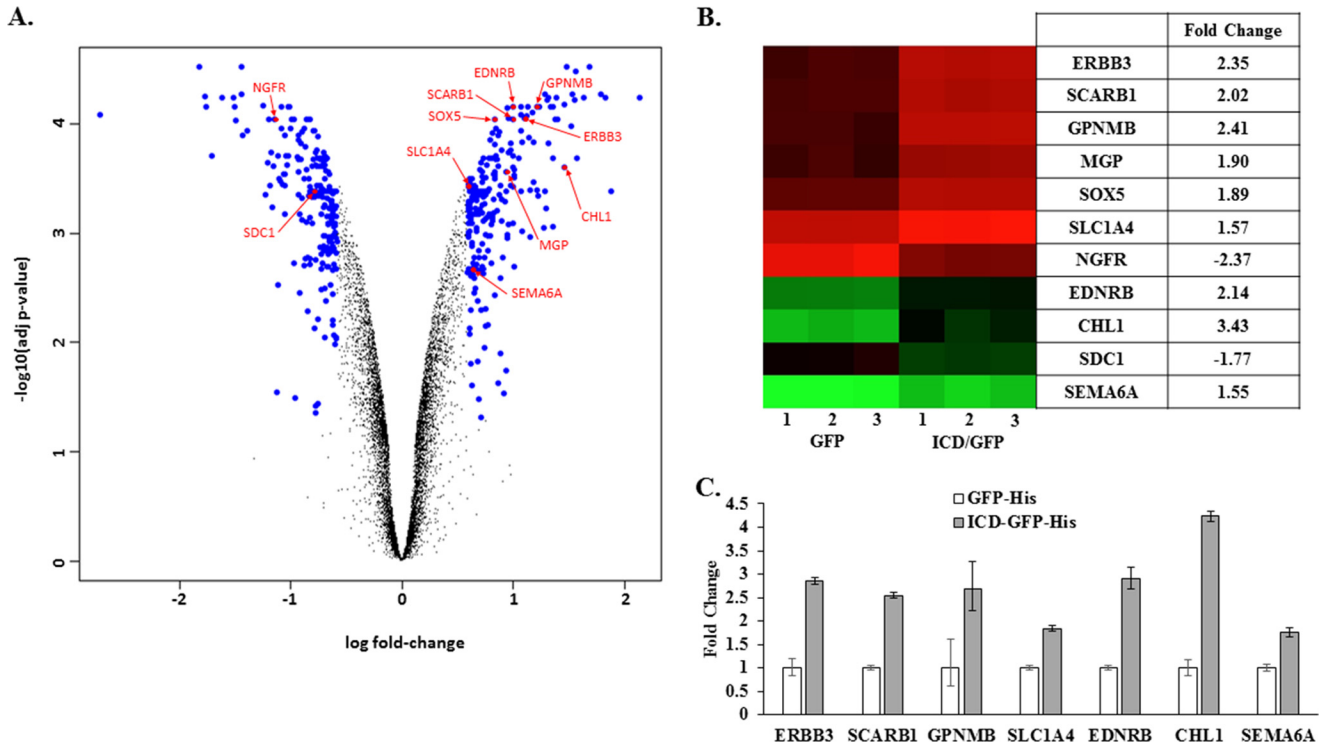

FIGURE 4. **Microarray identifies nine up-regulated MITF target genes due to teneurin-1 ICD overexpression.** *A*, *volcano plot* showing the 430 differentially regulated genes when the teneurin-1 ICD is overexpressed in BS149 cells compared with BS149 cells with overexpression of GFP only (-fold change >1.5; $p <$ 0.05). MITF target genes are marked in the plot. *B*, detailed view of the expression levels of the 11 MITF target genes in a *heat map*, where *bright green* means little or no expression and *bright red* means high expression. Nine genes are up-regulated, and two genes are down-regulated, with the -fold change indicated. *C*, quantitative RT-PCR confirmed the up-regulation of some of the MITF target genes. Values are normalized to TBP, and -fold change values compare overexpression of teneurin-1 ICD-GFP-His with GFP-His. *Error bars*, S.D.

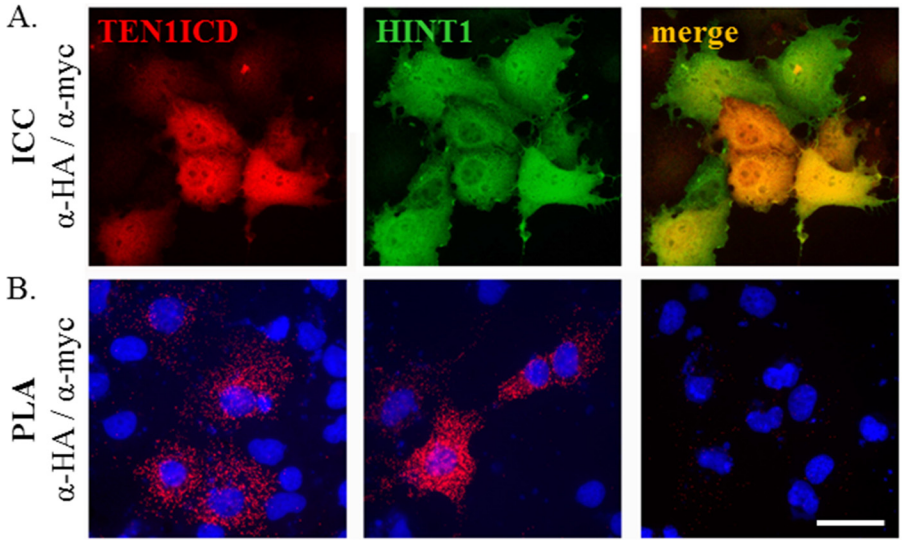

FIGURE 5. **Proximity ligation assay confirms the interaction between HINT1 and the TEN1-ICD.** *A*, immunocytochemistry (*ICC*) images of COS-7 cells co-transfected with TEN1ICD-HA and HINT1-MYC stained with anti-HA (*red*) and anti-MYC (*green*) and the merged channels showing co-expression in *yellow*. *B*, proximity ligation assay images of COS-7 cells co-transfected with TEN1ICD-HA and HINT1-MYC (*left* and *center images*) and COS-7 cells transfected only with HINT1-MYC as a negative control (*right image*); nuclei are stained with DAPI; *white bar*, 50 μm.

0.05), we obtained a list of 497 differentially regulated genes. Between the 430 genes differentially regulated by the TEN1-ICD and the 497 genes affected by MITF, there is an overlap of 42 genes that were either up- or down-regulated in both microarrays (Fig. 6*A*).

One of the overlapping genes is *GPNMB*, a target gene of MITF with a well described promoter that is directly bound by MITF (36). Therefore, we further investigated the effect of the TEN1-ICD on the expression of this particular gene. First, we could confirm by qPCR that MITF also regulates *GPNMB* in BS149 cells, showing a 4.14-fold increase in expression (Fig. 6*B*). To show a link of the TEN1-ICD and MITF via HINT1, HINT1 would have to influence MITF-regulated transcription. We therefore compared *GPNMB* transcript levels after co-

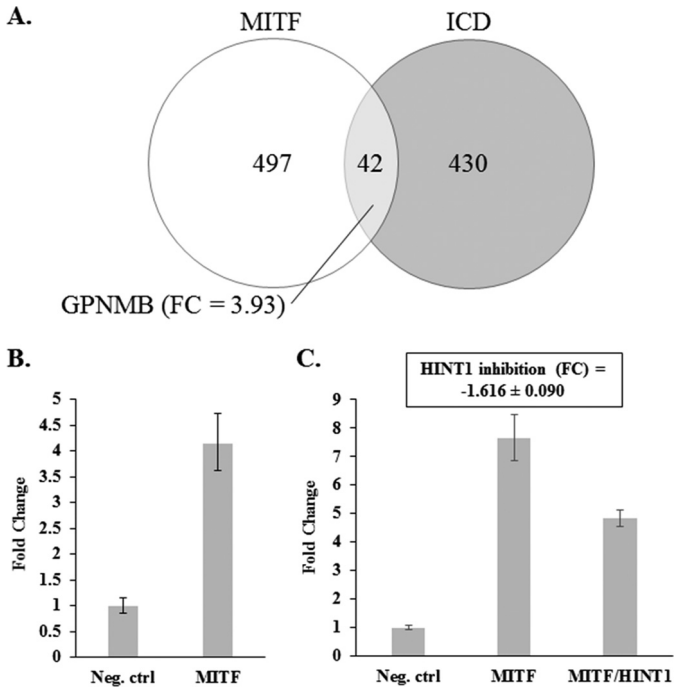

FIGURE 6. **MITF-induced overexpression of *GPNMB* is attenuated by co-transfection of HINT1.** *A*, a total of 497 genes are differentially regulated when MITF is overexpressed in BS149 cells. Of these genes, 42 are either up- or down-regulated due to both MITF and teneurin-1 ICD overexpression. One gene that is up-regulated in both microarrays is MITF target gene *GPNMB* (-fold change after MITF induction in *parentheses*). Overexpression of MITF-RFP-HA is compared with that of RFP-HA. Biological triplicates were used for the microarray. *B*, quantitative RT-PCR confirmed the up-regulation of *GPNMB* due to MITF overexpression. Values are normalized to TBP; -fold change value compares overexpression of MITF-RFP-HA with that of RFP-HA. *C*, quantitative RT-PCR results show a reduction of MITF-dependent transcription of *GPNMB* in the presence of HINT1. Values are normalized to *TBP*; -fold change values are compared with co-transfection of RFP-HA and CFP-C1 constructs (*Neg. ctrl*); the graph is representative of four separate experiments. The inhibition of *GPNMB* due to HINT1 compares the co-transfection of MITF-RFP-HA and HINT1-CFP-MYC with the co-transfection of MITF-RFP-HA and CFP-C1. Co-transfected cells were FACS-sorted before RNA isolation. *Error bars*, S.D.

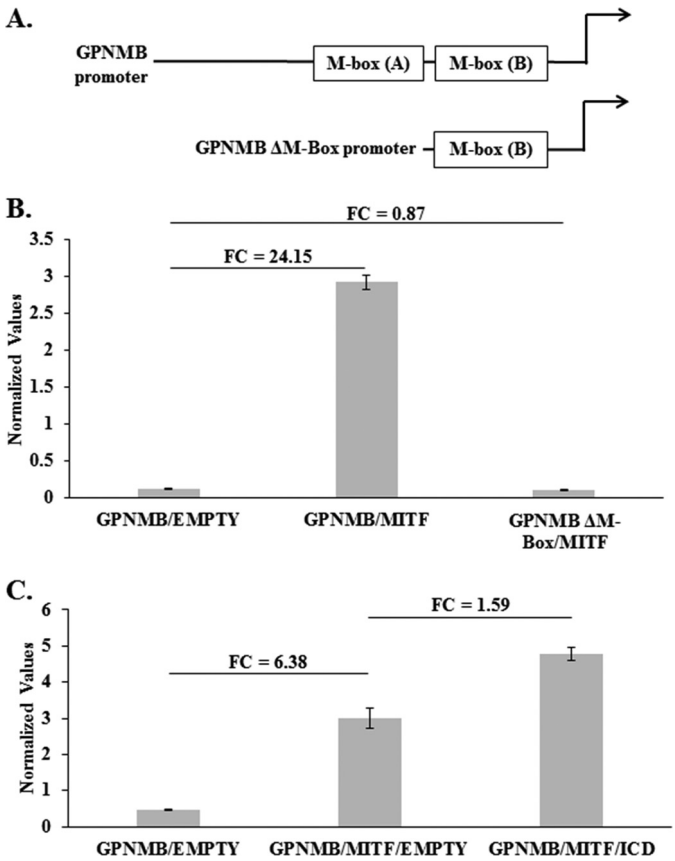

FIGURE 7. **The GPNMB promoter is induced by MITF in BS149 cells and further increased by overexpression of the teneurin-1 ICD.** *A*, diagram of the full-length *GPNMB* promoter and the *GPNMB* ΔM-box promoter, missing the M-box required for MITF-dependent regulation. *B*, SEAP assays show that MITF can induce the full-length *GPNMB* promoter activity, whereas the *GPNMB* ΔM-box promoter is not inducible. The transfection efficiency was normalized to luciferase assay values; -fold change values indicated by *FC above* the *bars* are compared with the full-length *GPNMB* promoter, co-transfected with empty pcDNA3.1 vector. *C*, SEAP assays show an increase of full-length *GPNMB* promoter activity when the teneurin-1 ICD is co-transfected with MITF, compared with MITF co-transfected with an empty pcDNA3.1 vector. The transfection efficiency was normalized to luciferase assay values, and -fold change values between the different conditions are indicated *above* the *bars*. *Error bars*, S.D.

transfection of cells with the MITF-RFP-HA and HINT1-CFP-MYC constructs. To make sure to analyze cells that overexpress both proteins, cells were FACS-sorted for expression of RFP and CFP before RNA isolation. Indeed, we saw a significant up-regulation of *GPNMB* transcripts when we transiently overexpressed the MITF-RFP-HA together with the empty control plasmid CFP-MYC, and this induction was attenuated by co-transfection with HINT1-CFP (Fig. 6*C*).

Finally, we wanted to investigate whether MITF directly influences *GPNMB* transcription in BS149 cells using promoter reporter experiments and whether this was affected by TEN1-ICD. To do this, we used two different promoter constructs of *GPNMB* in SEAP reporter gene assays: the full promoter and one missing the crucial MITF binding site M-box (*GPNMB* ΔM-box) as described previously (36) (Fig. 7*A*). Overexpressed MITF in BS149 cells strongly induced the full *GPNMB* promoter, with a 24.15-fold increase compared with the control, whereas the *GPNMB* ΔM-box promoter could not be induced by MITF (Fig. 7*B*). Thus, MITF directly binds to the *GPNMB* promoter and influences its transcription in BS149 cells. Next, we tested the influence of the TEN1-ICD on MITF-induced transcriptional activation of the *GPNMB* promoter reporter. This experiment showed that the TEN1-ICD further increases MITF-dependent transcription by 1.59-fold.

In summary, our results show that the transcriptional repressor HINT1 is a previously unknown interaction partner of teneurin-1, through which the TEN-1 ICD can influence MITF-dependent transcription, as depicted in the model presented in Fig. 8.

DISCUSSION

We propose a function for the ICD of teneurin-1 that is very similar to the Notch signaling pathway. Notch is a well studied type I transmembrane protein with a single-spanning transmembrane domain and an ICD that is much smaller in size than the ECD. The ICD can regulate transcription of several target genes by replacing repressors with other positive regulators in a transcription complex once it translocates to the nucleus (39).

In this study, we show that the teneurin-1 ICD can influence MITF-dependent transcription of *GPNMB* by binding to repressor HINT1. Although the ICDs of teneurins have been

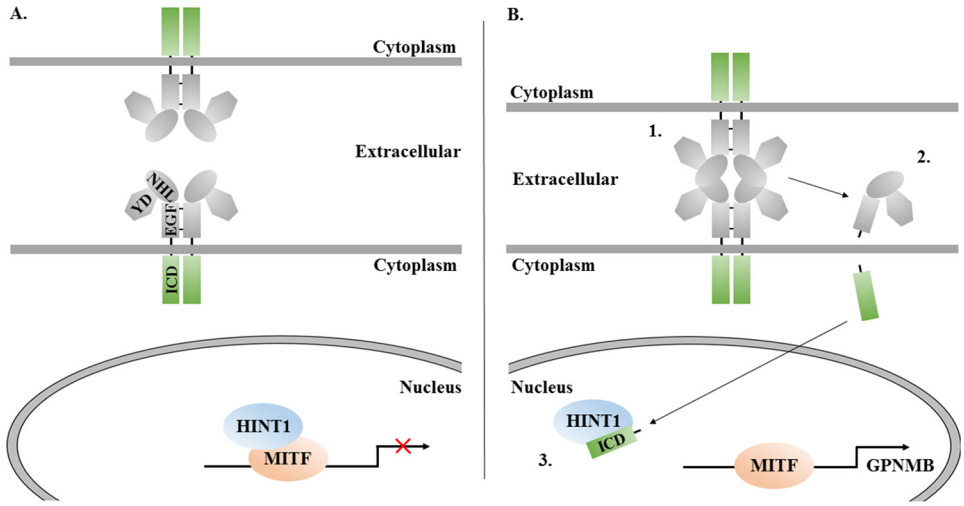

FIGURE 8. **The ICD of teneurin-1 regulates MITF-dependent *GPNMB* expression by competing for HINT1.** *A*, teneurin-1 ECD is not bound to an interaction partner, and the intracellular domain is not released from the plasma membrane. HINT1 in the nucleus inhibits MITF at the promoter of *GPNMB*. *B*, *1*, teneurin-1 interacts with a transmembrane protein of another cell. *2*, both the extracellular and intracellular domains are released from the membrane. The ICD translocates to the nucleus. *3*, the ICD competes for HINT1 binding, thus switching on MITF-dependent transcription of *GPNMB*.

implicated in transcriptional activity in the past (29, 32), here we are elucidating a new molecular mechanism to explain how a teneurin ICD can influence transcriptional activity. In our model, the ECD domain is released following homo- or heterophilic interaction, which is required for subsequently releasing the ICD.

Following its release, the ICD can translocate to the nucleus due to its predicted nuclear localization signal, as has previously been demonstrated in experimental studies (14, 29, 32). Here we have shown that the ICD can bind HINT1, thus switching on MITF-dependent transcription (Fig. 7). We showed this by using the MITF target gene *GPNMB* as an example, although there were 41 other genes differentially regulated by MITF and the TEN1-ICD. Most importantly, this highlights the potential of how teneurins can influence transcriptional regulation.

The mechanism of action of the TEN-1 ICD may be slightly different from Notch ICDs. Rather than replacing transcriptional repressors, recruiting positive regulators, and taking part in a transcriptional complex, the teneurin-1 ICD might regulate transcription by binding the transcriptional repressor and either releasing it from the transcription factor MITF or competing for binding to MITF. We are not ruling out the possibility that the TEN-1 ICD or the ICDs of the other teneurins have other modes of action, more like the Notch ICD. As we will discuss below, there are other interesting genes that might be regulated by the teneurin-1 ICD independent of MITF.

Although MITF-dependent transcription has mostly been studied in a melanocyte-specific context, other sites of expression like the retinal pigment epithelium have also been identified (40). Additionally, according to the Allen Mouse Brain Atlas (41), there is a weak MITF expression in the mouse olfactory bulb. However, MITF expression seems to have been rarely studied in the context of the central nervous system.

The expression of teneurin-1, HINT1, and GPNMB in the CNS has been studied more extensively. Unrelated studies suggest at least partially overlapping expression patterns of the three genes in the olfactory bulb, hippocampus, and cerebral cortex (14, 17, 42, 43). It will be very interesting to further explore the overlapping expression patterns of these genes in the CNS, including MITF, and to determine the function of the teneurin-1 ICD regulating MITF target genes like GPNMB. In the real-time qPCR screen, all tested glioblastoma cell lines expressed endogenous teneurin-1. In a recent review discussing teneurins in human tumorigenesis and malignancy, teneurin-2 and -4 were described as potential tumor suppressors or oncogenes (44). Teneurin-1 was not mentioned in the review, which may be due to a lack of data about the expression of this gene in tumors. *GPNMB* not only promotes invasiveness of glioma cells; it is also elevated in malignant glioblastomas. Taken together, this could be a first link of teneurin-1 to cancer and would make it a potential target in glioblastomas (45).

GPNMB is a type I transmembrane protein originally identified in human melanoma cells (45). Since then, its expression has also been identified in chondrogenesis (46), in differentiating osteoclasts and osteoblasts (46), and in normal and diseased brain tissue (43, 47). The function in the CNS is mostly unknown, although it is suggested to play a role in the stability of neurons and the immune/inflammatory response in the CNS (43). Interestingly, GPNMB also contains an RGD sequence in its ECD, which is likely to bind integrins (45). Integrins have also been studied in the context of axon guidance and neuronal connectivity (48). This leaves us with several potential functions of the teneurin-1 ICD regulating GPNMB expression. For one, GPNMB could regulate the stability of neurons once they have found their postsynaptic partner due to teneurin-1 homophilic binding. On the other hand, the capability of GPNMB to bind integrins could further specify or stabilize an interaction of the presynaptic neuron with its postsynaptic partner. Finally, we cannot exclude the possibility that our identified mechanism takes place in a non-neuronal context. Recent papers have identified teneurin-3 and -4 as important players in chondrogenic differentiation (49, 50). Although teneurin-1 has not been studied in chondrogenesis, the likely role of GPNMB as a key regulator in chondrogenesis could implicate a function of both proteins in this event.

Beyond the main aim of the study, we have also made several additional observations and findings. In addition to HINT1, we identified a total of 10 other novel interaction partners of the ICD by a yeast two-hybrid screen. Although we only focused on one of the interaction partners in the present work, each of the other proteins could be interesting to study in the context of teneurins. The three candidates brain-expressed X-linked 1 (BEX1), microtubule-actin cross-linking factor 1 (MACF1), and amyloid β A4 precursor protein-binding family B member 1 (APBB1) particularly stand out because they have all been implicated in neurite outgrowth. BEX1, for example, has also been shown to affect neuronal differentiation and cell cycle arrest, depending on its subcellular localization. One of the potential target genes of the TEN-1 ICD, nerve growth factor receptor (NGFR), seems to be essential in determining the localization of BEX1. In the nucleus, BEX1 inhibits cell cycle arrest, whereas in the cytosol, it competes with receptor-interacting protein 2 (RIP2) binding of NGFR, thus blocking the NF-κB pathway (51, 52). The teneurin-1 ICD could have a dual mode of action, by not only regulating transcription of *NGFR* but also aiding in the localization of BEX1 or working in a regulatory complex with BEX1. Another potential interaction partner, MACF1, contains an Src homology 3 domain and could be another link of teneurins to the cytoskeleton by binding to its polyproline-rich region (53). This interaction has previously been identified between teneurin-1 and CAP/Ponsin (29). It is also interesting that MACF1 has an important function in filopodia formation and axon elongation (54). Finally, APBB1 has been shown to bind the cleaved ICD of amyloid precursor protein and together translocate to the nucleus to regulate transcriptional activity in a complex (55). One possibility would be that the TEN1-ICD interacts with APBB1 in a similar mechanism and may regulate a different set of genes. APBB1 and amyloid precursor protein are also strongly expressed in the growth cones of neurons, where they are thought to regulate actin dynamics (56). However, the mechanism has not been resolved thus far. Because there is evidence that the TEN1-ICD can be linked to the cytoskeleton (29), it may also be involved with APBB1 and amyloid precursor protein in the growth cone.

In our whole transcriptome analysis of overexpressing the TEN-1 ICD in BS149 cells, we identified several hundred genes that were affected, many of which merit further analysis. For example, two of the potential target genes, close homolog of L1 (*CHL1*) and Ng-CAM-related cell adhesion molecule (*Nr-CAM*), are paralogs of the *Drosophila* gene neuroglian (*Nrg*). Whereas teneurins are responsible for proper connectivity and Nrg for synaptic stability in the neuromuscular junction (NMJ), both have a function in synaptic organization (8, 57). The ICDs could thus be involved in the regulation of Nrg in the NMJ of *Drosophila* or its orthologs in vertebrates. Interestingly, we also identified other target genes known to be inhibited by HINT1. For example, *TGFB2* is regulated by USF2 and CCND1 by β-catenin/TCF4, and both transcription factors have been shown to be inhibited by HINT1 (58). Hence, it is possible that the teneurin-1 ICD regulates not only MITF-dependent transcription via HINT1 but all HINT1-mediated inhibition of transcription.

Here we elucidated a novel mechanism of how the teneurin ICD can influence transcription. It is likely that additional mechanisms will be identified in the future, as this is a very diverse protein family with a wide range of important functions.

Acknowledgments—We thank Richard Tucker (University of California, Davis, CA) for critically reviewing the manuscript. We also thank Tim Roloff for helping with the analysis of the microarray data and Hubertus Kohler for performing the FACS experiments (both from Friedrich Miescher Institute, Basel, Switzerland).

REFERENCES

1. Baumgartner, S., and Chiquet-Ehrismann, R. (1993) Tena, a *Drosophila* gene related to tenascin, shows selective transcript localization. *Mech. Dev.* **40,** 165–176
2. Baumgartner, S., Martin, D., Hagios, C., and Chiquet-Ehrismann, R. (1994) Tenm, a *Drosophila* gene related to tenascin, is a new pair-rule gene. *EMBO J.* **13,** 3728–3740
3. Levine, A., Bashan-Ahrend, A., Budai-Hadrian, O., Gartenberg, D., Menasherow, S., and Wides, R. (1994) Odd Oz: a novel *Drosophila* pair rule gene. *Cell* **77,** 587–598
4. Minet, A. D., and Chiquet-Ehrismann, R. (2000) Phylogenetic analysis of teneurin genes and comparison to the rearrangement hot spot elements of *E. coli*. *Gene* **257,** 87–97
5. Oohashi, T., Zhou, X. H., Feng, K., Richter, B., Mörgelin, M., Perez, M. T., Su, W. D., Chiquet-Ehrismann, R., Rauch, U., and Fässler, R. (1999) Mouse ten-m/Odz is a new family of dimeric type II transmembrane proteins expressed in many tissues. *J. Cell Biol.* **145,** 563–577
6. Minet, A. D., Rubin, B. P., Tucker, R. P., Baumgartner, S., and Chiquet-Ehrismann, R. (1999) Teneurin-1, a vertebrate homologue of the *Drosophila* pair-rule gene ten-m, is a neuronal protein with a novel type of heparin-binding domain. *J. Cell Sci.* **112,** 2019–2032
7. Hong, W., Mosca, T. J., and Luo, L. (2012) Teneurins instruct synaptic partner matching in an olfactory map. *Nature* **484,** 201–207
8. Mosca, T. J., Hong, W., Dani, V. S., Favaloro, V., and Luo, L. (2012) Trans-synaptic Teneurin signalling in neuromuscular synapse organization and target choice. *Nature* **484,** 237–241
9. Drabikowski, K., Trzebiatowska, A., and Chiquet-Ehrismann, R. (2005) ten-1, an essential gene for germ cell development, epidermal morphogenesis, gonad migration, and neuronal pathfinding in *Caenorhabditis elegans*. *Dev. Biol.* **282,** 27–38
10. Mörck, C., Vivekanand, V., Jafari, G., and Pilon, M. (2010) *C. elegans* ten-1 is synthetic lethal with mutations in cytoskeleton regulators, and enhances many axon guidance defective mutants. *BMC Dev. Biol.* **10,** 55
11. Rubin, B. P., Tucker, R. P., Martin, D., and Chiquet-Ehrismann, R. (1999) Teneurins: a novel family of neuronal cell surface proteins in vertebrates, homologous to the *Drosophila* pair-rule gene product Ten-m. *Dev. Biol.* **216,** 195–209
12. Tucker, R. P., Martin, D., Kos, R., and Chiquet-Ehrismann, R. (2000) The expression of teneurin-4 in the avian embryo. *Mech. Dev.* **98,** 187–191
13. Tucker, R. P., Chiquet-Ehrismann, R., Chevron, M. P., Martin, D., Hall, R. J., and Rubin, B. P. (2001) Teneurin-2 is expressed in tissues that regulate limb and somite pattern formation and is induced *in vitro* and *in situ* by FGF8. *Dev. Dyn.* **220,** 27–39
14. Kenzelmann, D., Chiquet-Ehrismann, R., Leachman, N. T., and Tucker, R. P. (2008) Teneurin-1 is expressed in interconnected regions of the developing brain and is processed *in vivo*. *BMC Dev. Biol.* **8,** 30
15. Kenzelmann-Broz, D., Tucker, R. P., Leachman, N. T., and Chiquet-Ehrismann, R. (2010) The expression of teneurin-4 in the avian embryo: potential roles in patterning of the limb and nervous system. *Int. J. Dev. Biol.* **54,** 1509–1516
16. Ben-Zur, T., Feige, E., Motro, B., and Wides, R. (2000) The mammalian Odz gene family: homologs of a *Drosophila* pair-rule gene with expression implying distinct yet overlapping developmental roles. *Dev. Biol.* **217,** 107–120

17. Zhou, X. H., Brandau, O., Feng, K., Oohashi, T., Ninomiya, Y., Rauch, U., and Fässler, R. (2003) The murine Ten-m/Odz genes show distinct but overlapping expression patterns during development and in adult brain. *Gene Expr. Patterns* **3,** 397–405
18. Leamey, C. A., Merlin, S., Lattouf, P., Sawatari, A., Zhou, X., Demel, N., Glendining, K. A., Oohashi, T., Sur, M., and Fässler, R. (2007) Ten_m3 regulates eye-specific patterning in the mammalian visual pathway and is required for binocular vision. *PLoS Biol.* **5,** e241
19. Young, T. R., Bourke, M., Zhou, X., Oohashi, T., Sawatari, A., Fässler, R., and Leamey, C. A. (2013) Ten-m2 is required for the generation of binocular visual circuits. *J. Neurosci.* **33,** 12490–12509
20. Tucker, R. P., Beckmann, J., Leachman, N. T., Schöler, J., and Chiquet-Ehrismann, R. (2012) Phylogenetic analysis of the teneurins: conserved features and premetazoan ancestry. *Mol. Biol. Evol.* **29,** 1019–1029
21. Feng, K., Zhou, X. H., Oohashi, T., Mörgelin, M., Lustig, A., Hirakawa, S., Ninomiya, Y., Engel, J., Rauch, U., and Fässler, R. (2002) All four members of the Ten-m/Odz family of transmembrane proteins form dimers. *J. Biol. Chem.* **277,** 26128–26135
22. Beckmann, J., Schubert, R., Chiquet-Ehrismann, R., and Müller, D. J. (2013) Deciphering teneurin domains that facilitate cellular recognition, cell-cell adhesion, and neurite outgrowth using atomic force microscopy-based single-cell force spectroscopy. *Nano Lett.* **13,** 2937–2946
23. Boucard, A. A., Maxeiner, S., and Südhof, T. C. (2014) Latrophilins function as heterophilic cell-adhesion molecules by binding to teneurins: regulation by alternative splicing. *J. Biol. Chem.* **289,** 387–402
24. Kenzelmann, D., Chiquet-Ehrismann, R., and Tucker, R. P. (2007) Teneurins, a transmembrane protein family involved in cell communication during neuronal development. *Cell Mol. Life Sci.* **64,** 1452–1456
25. Wang, L., Rotzinger, S., Al Chawaf, A., Elias, C. F., Barsyte-Lovejoy, D., Qian, X., Wang, N. C., De Cristofaro, A., Belsham, D., Bittencourt, J. C., Vaccarino, F., and Lovejoy, D. A. (2005) Teneurin proteins possess a carboxy terminal sequence with neuromodulatory activity. *Brain Res. Mol. Brain Res.* **133,** 253–265
26. Lovejoy, D. A., Al Chawaf, A., and Cadinouche, M. Z. (2006) Teneurin C-terminal associated peptides: an enigmatic family of neuropeptides with structural similarity to the corticotropin-releasing factor and calcitonin families of peptides. *Gen. Comp. Endocrinol.* **148,** 299–305
27. Busby, J. N., Panjikar, S., Landsberg, M. J., Hurst, M. R., and Lott, J. S. (2013) The BC component of ABC toxins is an RHS-repeat-containing protein encapsulation device. *Nature* **501,** 547–550
28. Zhang, D., de Souza, R. F., Anantharaman, V., Iyer, L. M., and Aravind, L. (2012) Polymorphic toxin systems: Comprehensive characterization of trafficking modes, processing, mechanisms of action, immunity and ecology using comparative genomics. *Biol. Direct* **7,** 18
29. Nunes, S. M., Ferralli, J., Choi, K., Brown-Luedi, M., Minet, A. D., and Chiquet-Ehrismann, R. (2005) The intracellular domain of teneurin-1 interacts with MBD1 and CAP/ponsin resulting in subcellular codistribution and translocation to the nuclear matrix. *Exp. Cell Res.* **305,** 122–132
30. Tucker, R. P., and Chiquet-Ehrismann, R. (2006) Teneurins: a conserved family of transmembrane proteins involved in intercellular signaling during development. *Dev. Biol.* **290,** 237–245
31. Zheng, L., Michelson, Y., Freger, V., Avraham, Z., Venken, K. J., Bellen, H. J., Justice, M. J., and Wides, R. (2011) Drosophila Ten-m and filamin affect motor neuron growth cone guidance. *PLoS One* **6,** e22956
32. Bagutti, C., Forro, G., Ferralli, J., Rubin, B., and Chiquet-Ehrismann, R. (2003) The intracellular domain of teneurin-2 has a nuclear function and represses zic-1-mediated transcription. *J. Cell Sci.* **116,** 2957–2966
33. Razin, E., Zhang, Z. C., Nechushtan, H., Frenkel, S., Lee, Y. N., Arudchandran, R., and Rivera, J. (1999) Suppression of microphthalmia transcriptional activity by its association with protein kinase C-interacting protein 1 in mast cells. *J. Biol. Chem.* **274,** 34272–34276
34. Genovese, G., Ghosh, P., Li, H., Rettino, A., Sioletic, S., Cittadini, A., and Sgambato, A. (2012) The tumor suppressor HINT1 regulates MITF and β-catenin transcriptional activity in melanoma cells. *Cell Cycle* **11,** 2206–2215
35. Anastassiadis, K., Kim, J., Daigle, N., Sprengel, R., Schöler, H. R., and Stewart, A. F. (2002) A predictable ligand regulated expression strategy for stably integrated transgenes in mammalian cells in culture. *Gene* **298,** 159–172
36. Ripoll, V. M., Meadows, N. A., Raggatt, L. J., Chang, M. K., Pettit, A. R., Cassady, A. I., and Hume, D. A. (2008) Microphthalmia transcription factor regulates the expression of the novel osteoclast factor GPNMB. *Gene* **413,** 32–41
37. Schmittgen, T. D., and Livak, K. J. (2008) Analyzing real-time PCR data by the comparative C_T method. *Nat. Protoc.* **3,** 1101–1108
38. Hoek, K. S., Schlegel, N. C., Eichhoff, O. M., Widmer, D. S., Praetorius, C., Einarsson, S. O., Valgeirsdottir, S., Bergsteinsdottir, K., Schepsky, A., Dummer, R., and Steingrimsson, E. (2008) Novel MITF targets identified using a two-step DNA microarray strategy. *Pigment Cell Melanoma Res.* **21,** 665–676
39. Guruharsha, K. G., Kankel, M. W., and Artavanis-Tsakonas, S. (2012) The Notch signalling system: recent insights into the complexity of a conserved pathway. *Nat. Rev. Genet.* **13,** 654–666
40. Adijanto, J., Castorino, J. J., Wang, Z. X., Maminishkis, A., Grunwald, G. B., and Philp, N. J. (2012) Microphthalmia-associated transcription factor (MITF) promotes differentiation of human retinal pigment epithelium (RPE) by regulating microRNAs-204/211 expression. *J. Biol. Chem.* **287,** 20491–20503
41. Hawrylycz, M. J., Lein, E. S., Guillozet-Bongaarts, A. L., Shen, E. H., Ng, L., Miller, J. A., van de Lagemaat, L. N., Smith, K. A., Ebbert, A., Riley, Z. L., Abajian, C., Beckmann, C. F., Bernard, A., Bertagnolli, D., Boe, A. F., Cartagena, P. M., Chakravarty, M. M., Chapin, M., Chong, J., Dalley, R. A., Daly, B. D., Dang, C., Datta, S., Dee, N., Dolbeare, T. A., Faber, V., Feng, D., Fowler, D. R., Goldy, J., Gregor, B. W., Haradon, Z., Haynor, D. R., Hohmann, J. G., Horvath, S., Howard, R. E., Jeromin, A., Jochim, J. M., Kinnunen, M., Lau, C., Lazarz, E. T., Lee, C., Lemon, T. A., Li, L., Li, Y., Morris, J. A., Overly, C. C., Parker, P. D., Parry, S. E., Reding, M., Royall, J. J., Schulkin, J., Sequeira, P. A., Slaughterbeck, C. R., Smith, S. C., Sodt, A. J., Sunkin, S. M., Swanson, B. E., Vawter, M. P., Williams, D., Wohnoutka, P., Zielke, H. R., Geschwind, D. H., Hof, P. R., Smith, S. M., Koch, C., Grant, S. G., and Jones, A. R. (2012) An anatomically comprehensive atlas of the adult human brain transcriptome. *Nature* **489,** 391–399
42. Liu, Q., Puche, A. C., and Wang, J. B. (2008) Distribution and expression of protein kinase C interactive protein (PKCI/HINT1) in mouse central nervous system (CNS). *Neurochem. Res.* **33,** 1263–1276
43. Huang, J. J., Ma, W. J., and Yokoyama, S. (2012) Expression and immunolocalization of Gpnmb, a glioma-associated glycoprotein, in normal and inflamed central nervous systems of adult rats. *Brain Behav.* **2,** 85–96
44. Ziegler, A., Corvalán, A., Roa, I., Brañes, J. A., and Wollscheid, B. (2012) Teneurin protein family: an emerging role in human tumorigenesis and drug resistance. *Cancer Lett.* **326,** 1–7
45. Maric, G., Rose, A. A., Annis, M. G., and Siegel, P. M. (2013) Glycoprotein non-metastatic b (GPNMB): a metastatic mediator and emerging therapeutic target in cancer. *Onco Targets Ther.* **6,** 839–852
46. Abdelmagid, S. M., Barbe, M. F., Hadjiargyrou, M., Owen, T. A., Razmpour, R., Rehman, S., Popoff, S. N., and Safadi, F. F. (2010) Temporal and spatial expression of osteoactivin during fracture repair. *J. Cell Biochem.* **111,** 295–309
47. Tanaka, H., Shimazawa, M., Kimura, M., Takata, M., Tsuruma, K., Yamada, M., Takahashi, H., Hozumi, I., Niwa, J., Iguchi, Y., Nikawa, T., Sobue, G., Inuzuka, T., and Hara, H. (2012) The potential of GPNMB as novel neuroprotective factor in amyotrophic lateral sclerosis. *Sci. Rep.* **2,** 573
48. Myers, J. P., Santiago-Medina, M., and Gomez, T. M. (2011) Regulation of axonal outgrowth and pathfinding by integrin-ECM interactions. *Dev. Neurobiol.* **71,** 901–923
49. Murakami, T., Fukunaga, T., Takeshita, N., Hiratsuka, K., Abiko, Y., Yamashiro, T., and Takano-Yamamoto, T. (2010) Expression of Ten-m/Odz3 in the fibrous layer of mandibular condylar cartilage during postnatal growth in mice. *J. Anat.* **217,** 236–244
50. Suzuki, N., Mizuniwa, C., Ishii, K., Nakagawa, Y., Tsuji, K., Muneta, T., Sekiya, I., and Akazawa, C. (2014) Teneurin-4, a transmembrane protein, is a novel regulator that suppresses chondrogenic differentiation. *J. Orthop. Res.* **32,** 915–922
51. Carter, B. D. (2006) A Bex-cycle built for two. *EMBO Rep.* **7,** 382–384
52. Vilar, M., Murillo-Carretero, M., Mira, H., Magnusson, K., Besset, V., and

Ibáñez, C. F. (2006) Bex1, a novel interactor of the p75 neurotrophin receptor, links neurotrophin signaling to the cell cycle. *EMBO J.* **25,** 1219–1230
53. Margaron, Y., Fradet, N., and Côté, J. F. (2013) ELMO recruits actin cross-linking family 7 (ACF7) at the cell membrane for microtubule capture and stabilization of cellular protrusions. *J. Biol. Chem.* **288,** 1184–1199
54. Sanchez-Soriano, N., Travis, M., Dajas-Bailador, F., Gončalves-Pimentel, C., Whitmarsh, A. J., and Prokop, A. (2009) Mouse ACF7 and *Drosophila* short stop modulate filopodia formation and microtubule organisation during neuronal growth. *J. Cell Sci.* **122,** 2534–2542
55. Cao, X., and Südhof, T. C. (2001) A transcriptionally [correction of transcriptively] active complex of APP with Fe65 and histone acetyltransferase Tip60. *Science* **293,** 115–120
56. Sabo, S. L., Ikin, A. F., Buxbaum, J. D., and Greengard, P. (2003) The amyloid precursor protein and its regulatory protein, FE65, in growth cones and synapses *in vitro* and *in vivo*. *J. Neurosci.* **23,** 5407–5415
57. Enneking, E. M., Kudumala, S. R., Moreno, E., Stephan, R., Boerner, J., Godenschwege, T. A., and Pielage, J. (2013) Transsynaptic coordination of synaptic growth, function, and stability by the L1-type CAM Neuroglian. *PLoS Biol.* **11,** e1001537
58. Wang, L., Li, H., Zhang, Y., Santella, R. M., and Weinstein, I. B. (2009) HINT1 inhibits β-catenin/TCF4, USF2 and NFκB activity in human hepatoma cells. *Int. J. Cancer* **124,** 1526–1534
59. Cao, J. Y., Shire, K., Landry, C., Gish, G. D., Pawson, T., and Frappier, L. (2014) Identification of a novel protein interaction motif in the regulatory subunit of casein kinase 2. *Mol. Cell Biol.* **34,** 246–258
60. Proshkin, S. A., Shematorova, E. K., Souslova, E. A., Proshkina, G. M., and Shpakovski, G. V. (2011) A minor isoform of the human RNA polymerase II subunit hRPB11 (POLR2J) interacts with several components of the translation initiation factor eIF3. *Biochemistry* **76,** 976–980
61. Durrin, L. K., and Krontiris, T. G. (2002) The thymocyte-specific MAR binding protein, SATB1, interacts *in vitro* with a novel variant of DNA-directed RNA polymerase II, subunit 11. *Genomics* **79,** 809–817
62. Fanciulli, M., Bruno, T., Di Padova, M., De Angelis, R., Iezzi, S., Iacobini, C., Floridi, A., and Passananti, C. (2000) Identification of a novel partner of RNA polymerase II subunit 11, Che-1, which interacts with and affects the growth suppression function of Rb. *FASEB J.* **14,** 904–912
63. Cheung, H. N., Dunbar, C., Mórotz, G. M., Cheng, W. H., Chan, H. Y., Miller, C. C., and Lau, K. F. (2014) FE65 interacts with ADP-ribosylation factor 6 to promote neurite outgrowth. *FASEB J.* **28,** 337–349
64. Kypri, E., Christodoulou, A., Maimaris, G., Lethan, M., Markaki, M., Lysandrou, C., Lederer, C. W., Tavernarakis, N., Geimer, S., Pedersen, L. B., and Santama, N. (2014) The nucleotide-binding proteins Nubp1 and Nubp2 are negative regulators of ciliogenesis. *Cell Mol. Life Sci.* **71,** 517–538
65. Zheng, Y., and Lu, Z. (2013) Regulation of tumor cell migration by protein tyrosine phosphatase (PTP)-proline-, glutamate-, serine-, and threonine-rich sequence (PEST). *Chin. J. Cancer* **32,** 75–83
66. Li, W., Wang, C., Juhn, S. K., Ondrey, F. G., and Lin, J. (2009) Expression of fibroblast growth factor binding protein in head and neck cancer. *Arch. Otolaryngol. Head Neck Surg.* **135,** 896–901
67. Kolpakova, E., Wiedłocha, A., Stenmark, H., Klingenberg, O., Falnes, P. O., and Olsnes, S. (1998) Cloning of an intracellular protein that binds selectively to mitogenic acidic fibroblast growth factor. *Biochem. J.* **336,** 213–222
68. Tian, Y., Chang, J. C., Fan, E. Y., Flajolet, M., and Greengard, P. (2013) Adaptor complex AP2/PICALM, through interaction with LC3, targets Alzheimer's APP-CTF for terminal degradation via autophagy. *Proc. Natl. Acad. Sci. U.S.A.* **110,** 17071–17076
69. Gharesouran, J., Rezazadeh, M., Khorrami, A., Ghojazadeh, M., and Talebi, M. (2014) Genetic evidence for the involvement of variants at APOE, BIN1, CR1, and PICALM loci in risk of late-onset Alzheimer's disease and evaluation for interactions with APOE genotypes. *J. Mol. Neurosci.* **54,** 780–786
70. Du, Y., Meng, J., Huang, Y., Wu, J., Wang, B., Ibrahim, M. M., and Tang, J. (2014) Guanine nucleotide-binding protein subunit β-2-like 1, a new Annexin A7 interacting protein. *Biochem. Biophys. Res. Commun.* **445,** 58–63